DesignCon 2011

Examining the Impact of Power Structures on EM Model Accuracy

Jason R. Miller, Oracle Corp.
Jason.Miller@Oracle.Com, (781) 442-2774

Scott McMorrow, Teraspeed Consulting Group LLC
Scott@Teraspeed.Com, (401) 284-1827

Roger Dame, Oracle Corp.

Gustavo Blando, Oracle Corp.

Ashley Rebelo, LSI Corp.
Ash.Rebelo@LSI.Com , (610) 712-7234

Alejandro Lacap, LSI Corp.

Xiangyin Zeng, LSI Corp.

Istvan Novak, Oracle Corp.

Abstract

Three-dimensional models are often extracted with some implicit or explicit simplifying assumptions in order to reduce the solve time or improve accuracy. One common approach used with package extraction is to truncate the size of the package model in order to make the solve time more manageable. In this paper, we examine how the solver boundary conditions along with the model size impact the accuracy of popular commercial full-wave field solvers. We show that truncated models can introduce nonphysical resonances or miss resonances altogether. Recommendations will be made for problem set up to improve model accuracy.

Author Biographies

Jason R. Miller is a Principle Hardware Engineer at Oracle Corporation where he works on ASIC development, ASIC packaging, interconnect modeling and characterization, and system simulation. He has published over 40 technical articles on the topics such as high-speed modeling and simulation and co-authored the book "Frequency-Domain Characterization of Power Distribution Networks" published by Artech House. He received his Ph.D. in electrical engineering from Columbia University.

Scott McMorrow is President and Founder of Teraspeed Consulting Group. Mr. McMorrow is an experienced technologist with over 20 years of broad background in complex system design, interconnect & Signal Integrity engineering, modeling & measurement methodology, engineering team building and professional training. Mr. McMorrow has a consistent history of delivering and managing technical consultation that enables clients to manufacture systems with state-of-the-art performance, enhanced design margins, lower cost, and reduced risk. Mr. McMorrow is an expert in high-performance design and signal integrity engineering, and has been a consultant and trainer to engineering organizations world-wide.

Roger Dame is a Principle Hardware Engineer at Oracle Corporation where he works on mid-ranged servers, SI work in general, simulation, and lab work. He has 34 years of experience on analog, digital design and signal integrity work with DEC, Compaq, and HP. He received his B.S. in electrical engineering from CNEC.

Gustavo J. Blando is a Principle Hardware Engineer with over ten years of experience in the industry. Currently at Oracle Corporation, he is responsible for the development of new processes and methodologies in the areas of broadband measurement, high speed modeling and system simulations. He received his M.S. from Northeastern University.

Ashley Rebelo is a Staff Engineer in the packaging characterization group of LSI Corporation where he is responsible for Signal and Power integrity modeling of packaging interconnects. Prior to LSI he was Senior Member of Technical Staff in Agere System (formerly Lucent Technologies) where he was responsible for modeling and measurement validation of ASIC package and Interconnects. He holds a B.S in Electrical & Computer Engineering from Rutgers University and graduate studies at Lehigh University.

Alex Lacap earned his Bachelor's Degree in Electronics and Communications Engineering from University of the East in Manila, Philippines. He has a combined 23 years of extensive manufacturing and packaging experience and held 2 patents. His career started in 1987 in Texas Instruments as a wirebond process technician. In 1991, he was a design engineer of leadframes and BGA packages. In his senior years in TI, he was the department head of a front-of-line engineering services team. In 1999, he was promoted Member, Group Technical Staff handling electrical modeling under New Product Development group. He joined LSI Logic (now LSI Corporation) in 2001 as a Signal Integrity engineer inside Packaging group. Alex is an avid karaoke singer and loves gardening and hiking.

Xiangyin Zeng is a Staff Engineer at LSI with focus on package model extraction, package modeling methodology development, PDN analysis and methodology development. He has worked for Intel as an SI staff engineer for 7 years and achieved top invention award in 2007. He has co-authored 7 papers on IEEE transactions and letters, co-authored 10 US patents. He received his Ph.D. in Electrical Engineering from University of Science & Technology of China, and received the prestigious Presidential Award from the Chinese Academy of Sciences in 2000.

Istvan Novak is a Senior Principle Engineer at Oracle. Besides signal integrity design of high-speed serial and parallel buses, he is engaged in the design and characterization of power-distribution networks and packages for mid-range servers. He creates simulation models, and develops measurement techniques for power distribution. Istvan has twenty plus years of experience with high-speed digital, RF, and analog circuit and system design. He is a Fellow of IEEE for his contributions to signal-integrity and RF measurement and simulation methodologies.

1 Introduction

Three-dimensional models are often extracted with some implicit or explicit simplifying assumptions in order to reduce the solve time or improve accuracy. For example, package models, which can contain many fine geometric details, are often truncated from the larger package database so that they contain only a handful of differential pairs (see Figure 1). It is assumed that the return current and fields at high frequencies will primarily exist in the vicinity below and/or above the trace on the planes including any vias in the signal path. In this approach, power-ground structures, which often extend across large swaths of the package, are either removed completely or truncated to help with solve time. In this paper we show how these simplifying assumptions can introduce nonphysical resonances or miss resonances altogether.

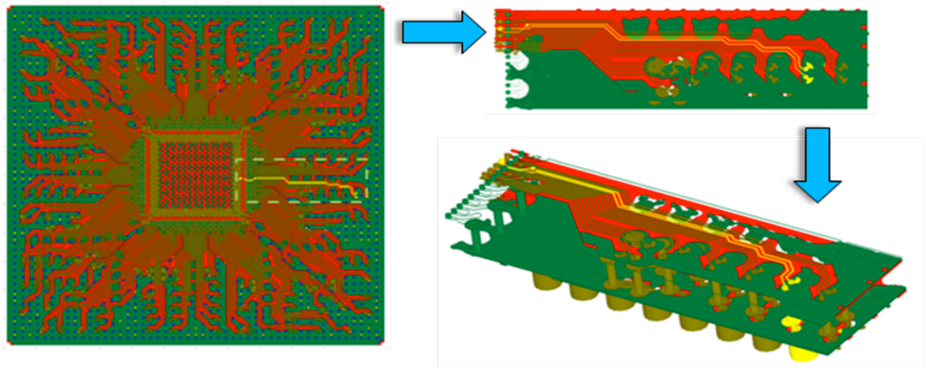

Figure 1 Illustration showing a common procedure for creating a package model. In the first step the package design is truncated to create a smaller design file. The final model that is analyzed contains a handful of differential pairs and the plane extents are now defined by the cut locations.

In the first part of the paper we briefly review the theory of cavity resonances and discuss ways that cavities can get excited by signals. We then look at cavity and signal interaction. In particular, we see how a signal can excite cavity resonances and how the presence of ground vias shifts these resonances. In the next section we examine the accuracy of models extracted with commercial field solvers and focus on the impact of boundary conditions on the accuracy of these models. Finally, we show measurement to simulation correlation data on a coupled differential via structure. Although the principles we discuss in this paper are general, an emphasis is placed on package models as oppose to PCB models.

2 Background

In this section we look at the behavior of plane cavities and ways of exciting a cavity. In the first sub-section we review the theory of plane cavity resonances. In the second sub-section we look at how plane cavity resonances can be excited by signals.

2.1 Plane Cavity Resonances

Open-edge rectangular plane pairs, like transmission lines, resonate at multiples of half wavelengths (e.g., 1, 3/2, 2, 5/2, ...). At these frequencies the self-impedance profile exhibits peaks. These peaks are often called parallel resonances due to the fact that the impedance of a lossless tank circuit tends towards infinity at resonance. Also like transmission lines, there are dips in the impedance profile between the peaks, but not necessarily at multiples of quarter wavelengths (e.g., 3/4, 5/4, 7/4, 9/4, ...). The first of these resonances, i.e., the fundamental, is often referred to as the series resonance, due to the fact that the impedance of a series circuit at resonance, approaches its series resistance loss. The overall impedance profile is spatially dependent. The parallel resonances, for example, may be suppressed where there is modal cancellation. As the frequency increases, the magnitude ratio of subsequent peaks and dips diminishes due to two reasons: higher-order modes follow each other with lower relative frequency spacing and also due to frequency dependent losses. The amplitude of these resonances can be reduced by decreasing either the metal or dielectric thickness [1].

Figure 2 shows the simulated impedance of a 10 inch x 10 inch plane pair as measured from the center of the board. The impedance across the plane was calculated as follows [2]:

$$Z_{ij}(\omega) = Z(\omega)\sum_{n=0}^{\infty}\sum_{m=0}^{\infty}\frac{\chi_{mn}^{\ 2}}{w_x w_y\left(k_{xm}^{\ 2} + k_{yn}^{\ 2} + Z(\omega)Y(\omega)\right)} f(x_i, y_i, x_j, y_j) \qquad (1)$$

The surface impedance across the plane is shown for the three frequency points marked on the self impedance curve. At low frequencies we notice that the impedance is the same across the plane pair, dictated by the static capacitance. Looking at the second frequency point, we see that the series resonance frequency will change in frequency depending on where you measure it on the plane because the plane inductance at lower frequencies varies with location. The parallel resonance frequency will largely be fixed because this peak is dictated by the dimension of the plane. However, in this case, the first modal resonance is suppressed due to modal cancelation at the probing location; the second parallel resonance is shown but there are locations on the plane where it too would be suppressed.

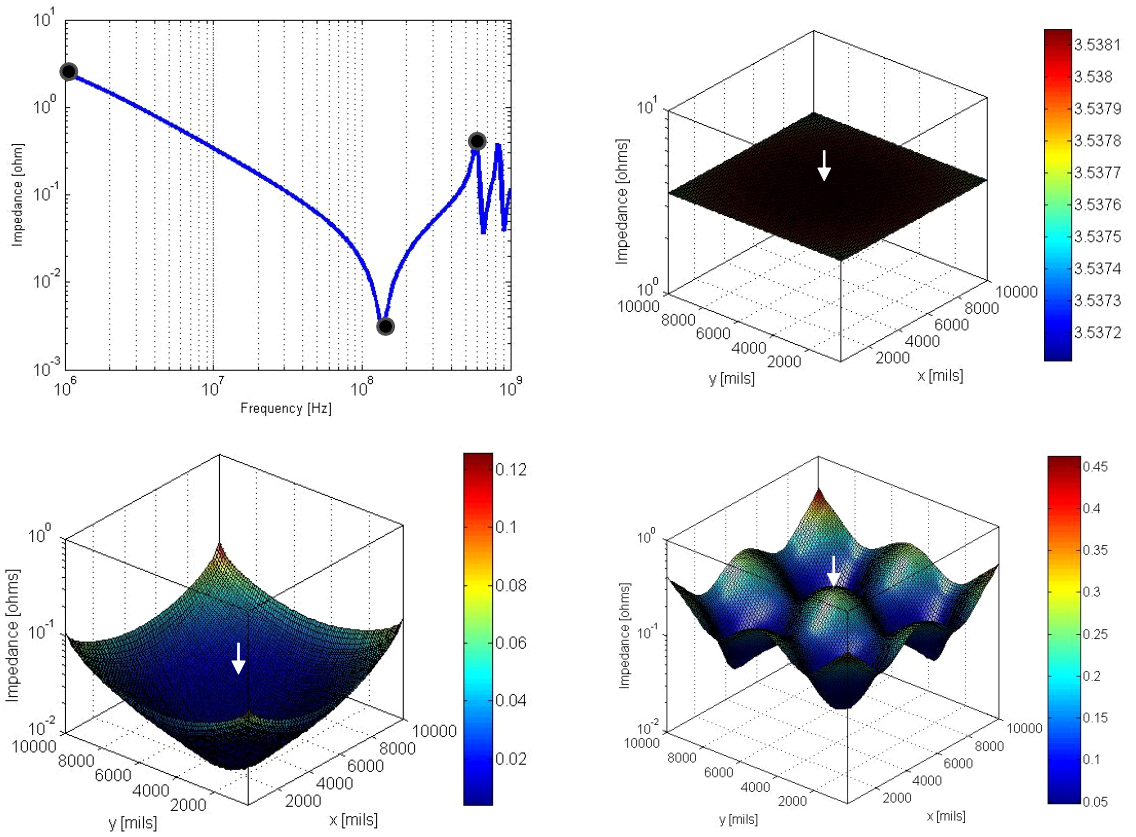

Figure 2 Frequency and spatial dependence of the impedance of a 10 inch x 10 inch plane pair. *Top Left:* Simulated self-impedance of a 10 inch square board as measured from the center of the board. *Top Right:* Plane impedance at 1 MHz. *Bottom Left:* Plane impedance at series resonance frequency. *Bottom Right:* Plane impedance at first parallel resonance frequency. There are no ground or signal vias on the plane.

2.2 Cavity Excitations by Signals

Cavities (e.g., power-ground or ground-ground planes) can be excited in a number of ways allowing energy to propagate in TEM parallel-plane waveguide mode.

One way to excite a cavity is to scatter energy off a discontinuity in the signal path, such as a plane split [3]. Consider a two-port network. If a power wave is injected into Port 1, part of the power will be reflected back to Port 1, the remainder will propagate through to Port 2 (transmitted) and part of this transmitted wave can be lost due to dissipated losses or radiation losses. This can be written as:

$$P_{port-2} = P_{port-1} - P_{loss} - P_{radiated} \qquad (2)$$

From the perspective of Port 1, the power radiated into the plane cavity will look like additional loss at that frequency. This radiated power increases crosstalk to neighboring traces or reflect again off of other boundaries.

In this paper we will focus on excitation of cavities from signal vias transitioning through cavities. A commonly held belief is that if you control and match the impedance of a via as it transitions, the fields will be contained, thus limiting the cavity excitation. In the following paragraphs we explore the truth and feasibility of this statement.

Investigations of so-called via "impedance" tend to focus on the problem of signals propagating through planes as a holistic approach, finding a geometry that produces the "best" input to output impedance match across a wide bandwidth. Additional insight, however, can be gained by viewing plane cavity traversal as the perturbation of a uniform transmission line by a repetitive loading structure, where each cavity section represents an additional loaded element. When viewed in this way, a single loaded cavity section can be viewed independent of other elements in a via chain. This assumption is built into package solvers utilizing the method of hybrid modal decomposition [9], however, the underlying electromagnetic assumptions in the plane traversal region are rarely exposed to public view.

To facilitate this investigation, a unique via transition modeling method, as shown in Figure 3, was devised to investigate the impact of cavity traversal on signal propagation through vias. The problem is divided into two section types. First, a uniform signal/ground via transmission line section was built with electromagnetic wave port launches. An array of signal and ground vias forms a well-defined TEM transmission line with a field pattern that is dependent entirely on via geometry and has known characteristics. Ground planes forming a cavity are then attached to the center of the transmission line, utilizing filaments that connect the via ground structure to the planes. This structure allows for systematic parametric investigations of various plane apertures, signal/ground via geometries, and types of transitions.

Initially a square via array pattern with 0.25 mm via diameter on a 1 mm pitch was built, crossing a 800 micron thick 8 mm x 8 mm plane cavity. The plane clearance opening was then parameterized and swept from 0.75 mm to 4 mm in diameter to observe impact on characteristic impedance. The via transmission line characteristic impedance is observed to be 69.3 ohm. Observation of this via field pattern clearly shows that significant field energy is not contained by the ground structure, and that an e-field strength of a least -20 dB leaks from containment. If no other structure intervenes in the signal propagation path through these vias, then this field pattern will be maintained from port 1 to port 2. However, if these vias are passed through a ground cavity, some of the signal energy will be coupled to the ground planes, becoming available for cavity modal excitation.

The TDR profile of a wideband Gaussian pulse excitation was used to evaluate the impact of cavity mode excitation on "via impedance". A clearance diameter of 2.6 mm is the smallest size that produces negligible via impedance disturbance while propagating a

50 GHz Gaussian pulse. Reliable manufacturing requires smaller clearance holes to be used, causing significant repetitive disturbance of the signal fields, and increased coupling into the plane cavity. Any electromagnetic field energy that is not contained by the via ground structure may then be radiated into the cavity. To the signal path this shows up as an impedance disruption and loss of signal amplitude. To the cavity this energy appears in the form of modal voltage transients, crosstalk injection into other signal vias, and edge radiation.

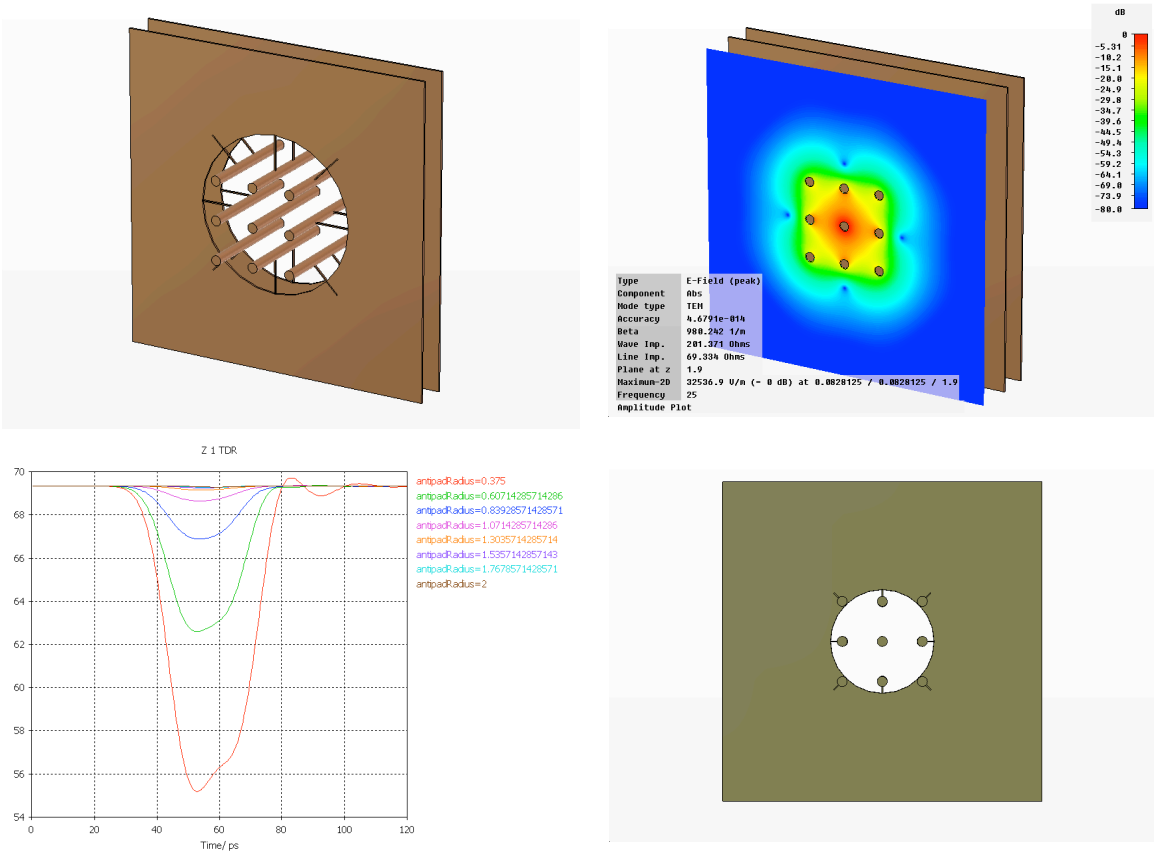

Figure 3 Modeling of via signal propagation with plane cavity loading. *Top Left:* Modeled parametric structure. *Top Right:* 2D Port TEM E-field distribution . *Bottom Left:* TDR showing impact of vias crossing plane with various plane clearances. *Bottom Right:* 2.6 mm plane clearance diameter shows negligible impedance disturbance.

3 Signal and Plane Cavity Interactions

In this section, we will focus on excitations of cavities due to signal via transitions.

Vias provide the means of transmitting energy between different layers in a board or a package. This injected current will transverse cavities. If the current is not perfectly contained, a portion of the injected energy will propagate in the cavity in all directions encountering different types of obstacles including other vias. These vias will act as

return paths for the signal and help to contain the plane waves. If plane waves encounter an open plane boundary, such as an edge of the board, the plane wave can be reflected back into the cavity, creating resonances, or transmitted (e.g. radiated), or even terminated (e.g. dissipative edge termination).

Figure 4 shows the simulation results for a 5-2-5 package substrate; the plane outline is 450 mils x 450 mils. A single via transitions from the top of the stack to the bottom (i.e., no stub) and is positioned approximately in the middle of the x-y plane; the lead-in and lead-out traces are routed on the build-up layers in a stripline configuration. The planes are stitched together at the corners of the planes. The structure was simulated in Ansoft SIwave using the solver settings that were used on a similar geometry and found to correlate to measurement (see Section 5).

The s-parameter plot shows two major insertion loss dips at 4.4 GHz and 16.7 GHz. The accompanying surface plots show the voltage difference across the core layer of the substrate. At frequencies below the resonance frequency of the plane, the voltage difference across the core layer is near zero (blue color). The first dip in the insertion loss profile corresponds to the half-wave resonance of the plane (4.4 GHz) along the diagonal dimension of the plane and the second major dip at 16.7 GHz corresponds to the second full-wave resonance. The first full-wave resonance is suppressed because of the location of the via in the plane (although due to the slightly offset via placement within the square plane, the dip is still visible at about 9 GHz). We observe that the simulated response is a product of via position within the cavity and the plane cavity natural standing waves.

In the following sections we look at the impact of ground vias placed either in the vicinity of the primary signal via or further away in the plane cavity.

3.1 Modifying the Cavity Modal Frequencies

Figure 5 shows the same simulation case as shown in Figure 4 but now a number of stitching vias have been added to the far corner. The new s-parameter plot shows a higher half-wave resonance frequency compared to Figure 4 (6.12 GHz versus 4.4 GHz) as the effective diagonal dimension of the plane has been reduced due to the presence of stitching vias. We can view stitching vias as *shorted* plane boundaries (as opposed to *open* plane boundaries); in either case, the boundary still provides a full reflection. The resonance frequencies of the cavity are dictated by these open and shorted boundaries.

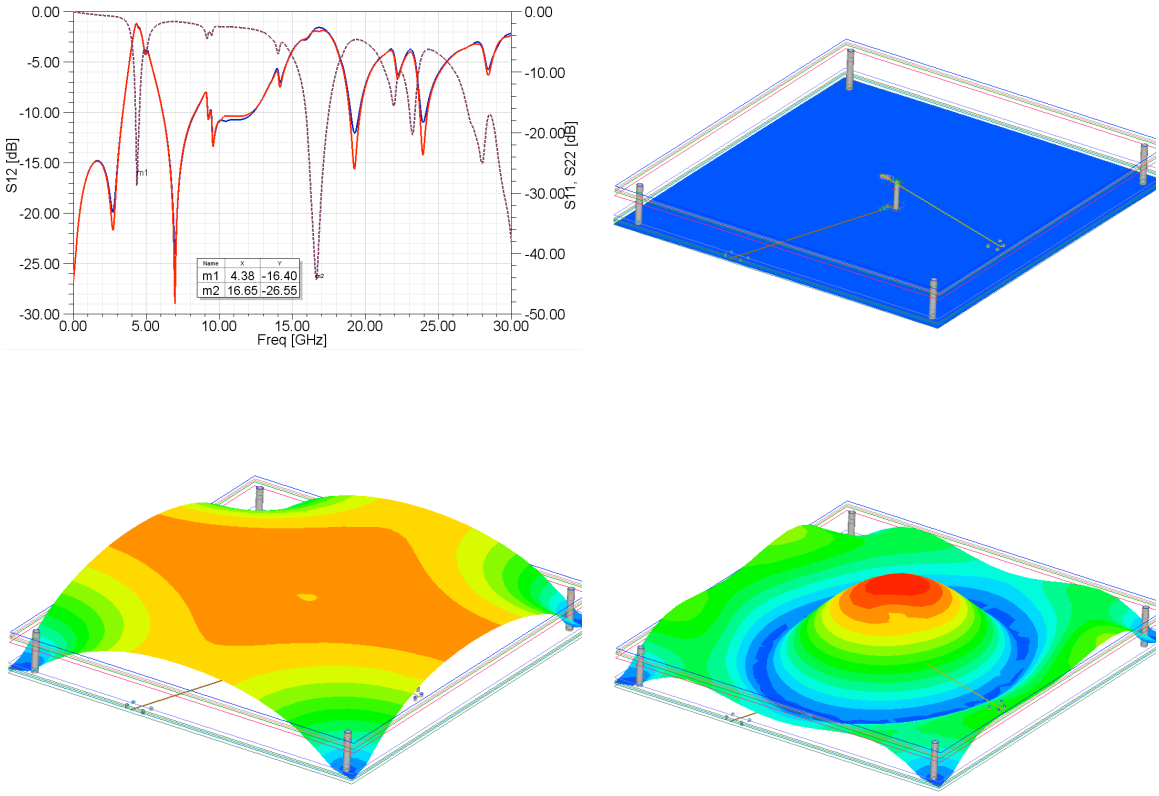

Figure 4 Cavity excitations by a via transition through a package substrate. *Top Left:* Simulated s-parameters. *Top Right:* Voltage difference on plane pair is close to zero up to ~4 GHz. *Bottom Left:* Voltage difference at insertion loss dip (~4.4GHz). *Bottom Right:* Voltage difference on plane at 16.7 GHz. The slight asymmetry in the plots is due to the via being slightly offset from the center of the plane.

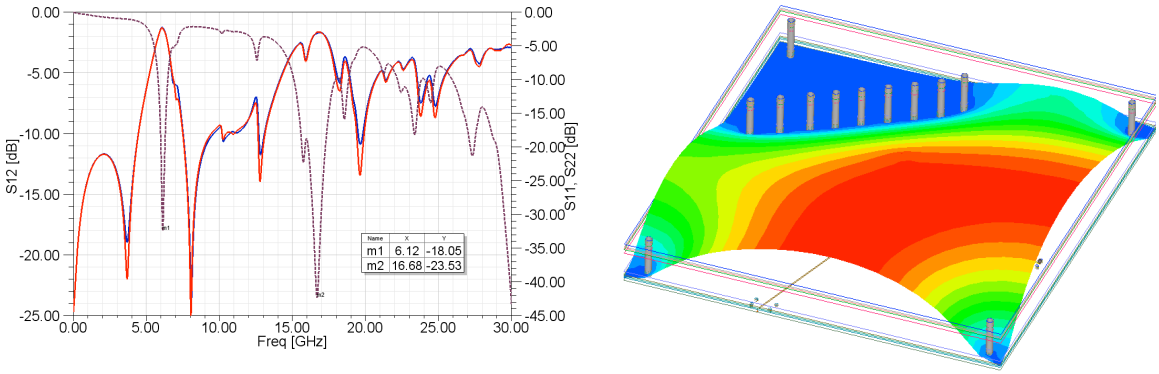

Figure 5 Cavity excitations by a via transition through a package substrate with stitching vias. *Left:* Simulated s-parameters. *Right:* Voltage difference on plane pair at half-wave resonance (6.12 GHz).

Plane perforations due to, for example, other signal vias, will also shift the modal resonances of the plane cavity. However, these cutouts don't, in general, prevent the series and parallel resonances of the plane cavity from being established.

As we cut holes on planes, the static plane pair capacitance decreases while the loop inductance increases. The increased loop inductance offsets the reduction of plane capacitance pushing the series resonance to a lower-frequency. In Figure 6 the series resonance is in fact pushed to a lower frequency although the high-Q of the series resonance makes the visual comparison misleading. Figure 6 (Bottom Left) shows that the half-wave resonance frequency is still established and similar to what we see in Figure 4.

Based on the results shown in Figure 6, we can conclude that the first parallel resonance is also pushed to a lower frequency indicating the plane has an effective larger size as the waves have to travel around the holes to get to the boundary. Similar findings were reported in [4]. Note that the parallel resonance is not a strong function of the plane perforation or cutouts; an earlier study showed that with more than 60% of the copper area removed in the center of a 4 inch x 6 inch plane, the parallel resonance was only shifted down by about 30% [5].

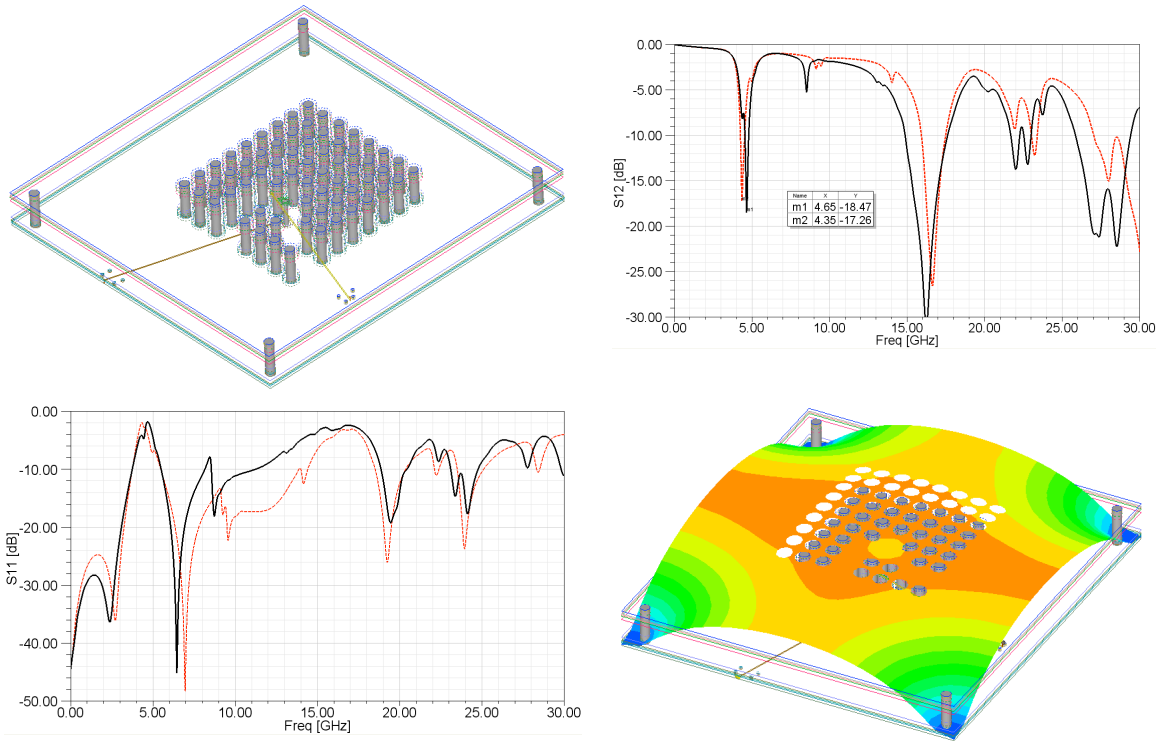

Figure 6 Cavity excitations by a via transition through a package substrate with a perforated pin field region. *Top Left:* Problem geometry. *Top Right:* Simulated insertion loss parameter compared to solid plane case. The black traces are with the perforations. *Bottom Left:* Simulated return loss parameter compared to solid plane case. *Bottom Right:* Voltage difference on plane at the half-wave resonance.

3.2 Containment Vias

Figure 7 (Left) shows an example of a signal via surrounded by ground vias on a 1 mm pitch – in real packages, these unit cells may repeat to create a BGA pin field. As we saw earlier in Figure 4, the plane cavity has a diagonal half-wave resonance at 4.4 GHz. However, Figure 7 shows that we do not excite that mode as the surrounding ground vias contain all of the return current at that frequency. In fact, the insertion loss profile is now smooth to about 16 GHz while the return loss hovers around -20dB.

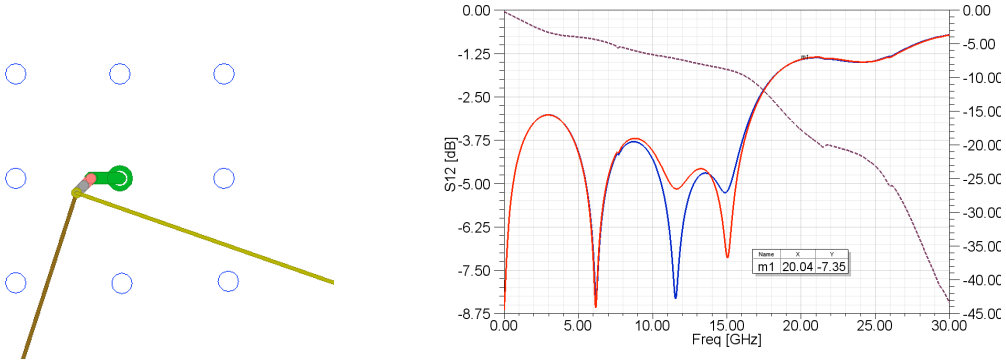

Figure 7 Cavity excitations by a via transition through a package substrate with containment vias. *Left:* Problem geometry. *Right:* Simulated s-parameters.

The first major resonance that occurs at 20 GHz in Figure 7 is the result of the new boundary created by the ground vias themselves: the signal via surrounded by grounds acts as an shorted electrical boundary (versus a plane edge which is an open boundary). It reflects all the energy from the signal via and creates a half-wave resonance based on the diagonal dimension of the closed boundary. This is shown in Figure 8 (Left). To increase the usable bandwidth of the signal, a finer pitch pin field may be used (say 0.8 mm); in this case, this would push the usable bandwidth of the signal out by 20%. Note that a differential pair surrounded by grounds would lower this resonance by 20% since the maximum distance between grounds increases.

The tightly stitched grounds in Figure 7 contain the fields to well above 30 GHz. If, instead, one of those vias is missing due to an irregular ball grid array pattern, for example, the results are much different. Figure 8 (Right) shows the voltage surface plot at approximately 30 GHz for this case. At that frequency we observe fields escaping where the via has been removed. In fact, due to the missing via, a new resonance is introduced, formed between the via and the plane boundary.

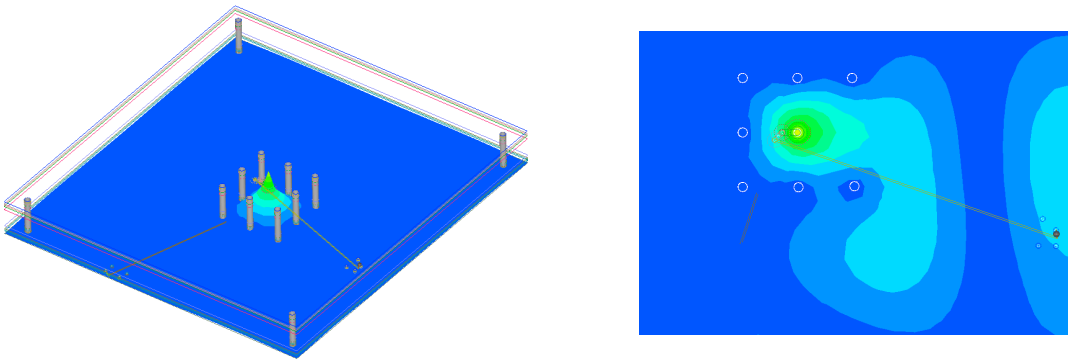

Figure 8 Voltage surface plots for a via transition through a package substrate with containment vias. *Left:* First resonance at 20 GHz with all vias intact. *Right:* Surface voltage with a missing containment via at 30 GHz.

In order to further understand field containment by ground vias, a simulation was run in CST MWS using a simple two stack board with small ground blades to short the planes arranged in a square pattern around the center of the board where the excitation port was located [4]. The blade separation was 20 mils and each side of the wall was 80 mils in length. In the first run, an absorbing boundary condition was used.

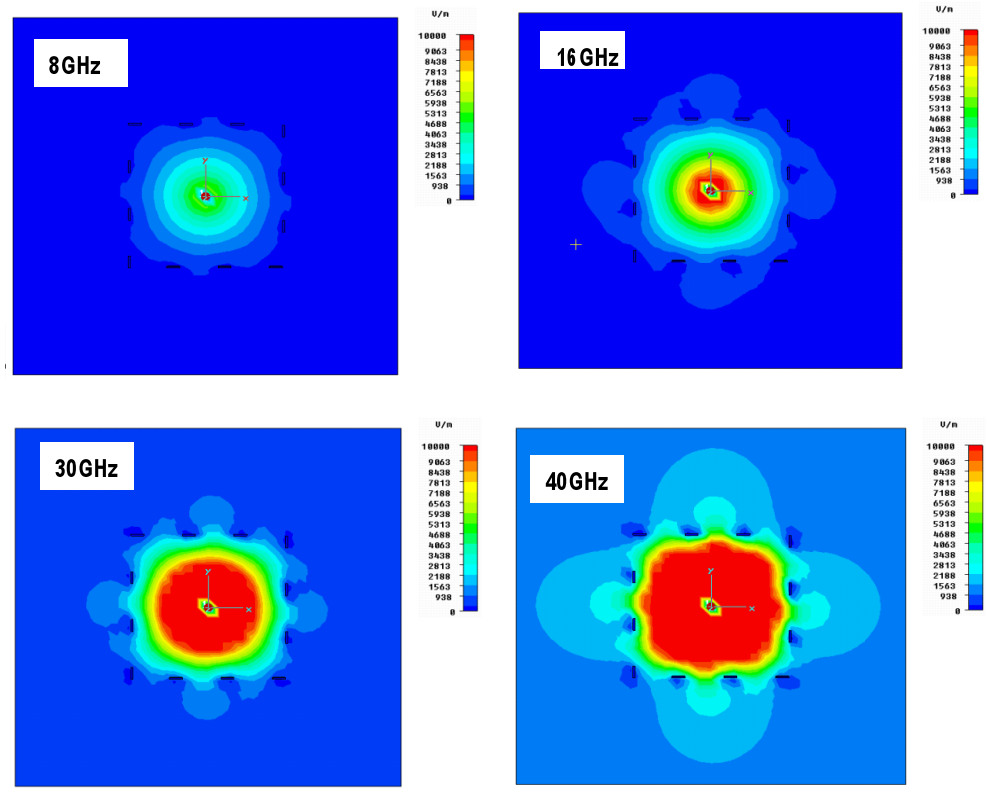

Figure 9 Electric field distribution at different frequencies. *Top Left:* 8 GHz. *Top Right:* 16 GHz. *Bottom Left:* 30 GHz. *Bottom Right:* 40 GHz. An absorbing boundary was used at the plane edge.

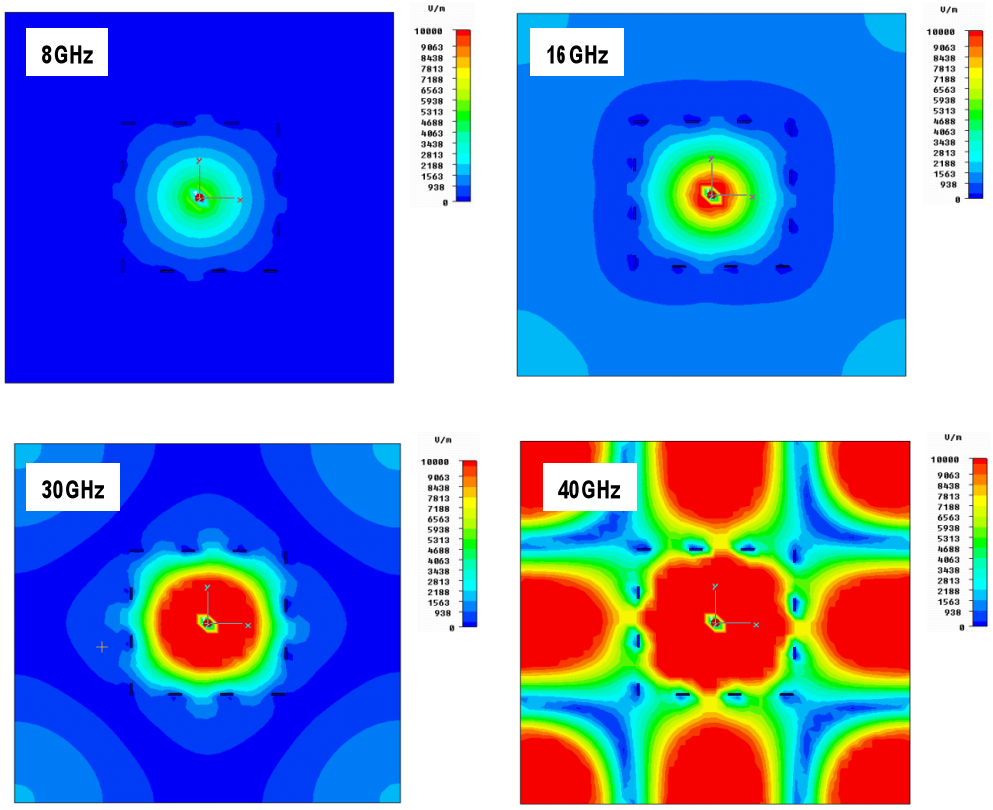

Figure 10 Electric field distribution at different frequencies. *Top Left:* 8 GHz. *Top Right:* 16 GHz. *Bottom Left:* 30 GHz. *Bottom Right:* 40 GHz. An magnetic boundary was used at the plane edge.

Figure 9 plots the fields at 8 GHz, 16 GHz, 30 GHz, and 40 GHz. The wall is successful at containing the fields at 8 GHz. At 40 GHz we see that the 20 mil ground blade separation leaks fields through the blades. Figure 10 shows the same simulation except now a magnetic boundary is used at the edge of the planes. As the frequency increases, we observe that the fields penetrating the via blades create standing wave patterns due to the reflection off the magnetic boundary. If the planes are not properly terminated, these standing wave patterns can cause peaks and dips in the insertion and return loss at the excitation port. Furthermore, anywhere on the board where there is a peak in the electric field magnitude, there would be additional coupling. This will be discussed in the next section in more detail.

3.3 Non-locality of Fields

Simulations were performed on multiple via geometries using the structure in Figure 3 using a fixed plane clearance diameter of 0.75 mm, which is typically the largest that can be accommodated in manufacturing on a 1 mm pitch device. The natural characteristic impedance and field distributions for 16, 8, 6, and 4 ground coaxial ground structures is shown in Figure 11. At near maximum field containment, characteristic impedance of the transmission line is 63.4 ohm, and there is negligible field leakage above -60 dB. With four ground vias, the natural impedance has increased to 71.4 ohm, and there is significant field non-locality. It is exactly this non-containment of propagating fields that leads to excitation of the planar cavities and system wide field non-locality. That is, a signal propagating through one set of signal/ground vias, may pop up in "Whack-A-Mole" fashion, a significant distance away in another signal via. Although the coupling appears as "noise" on ground and power planes, and insertion loss in the primary signal path, this non-localized via-to-via coupling appears as near and far end crosstalk on the coupled via, which can be a much more significant problem.

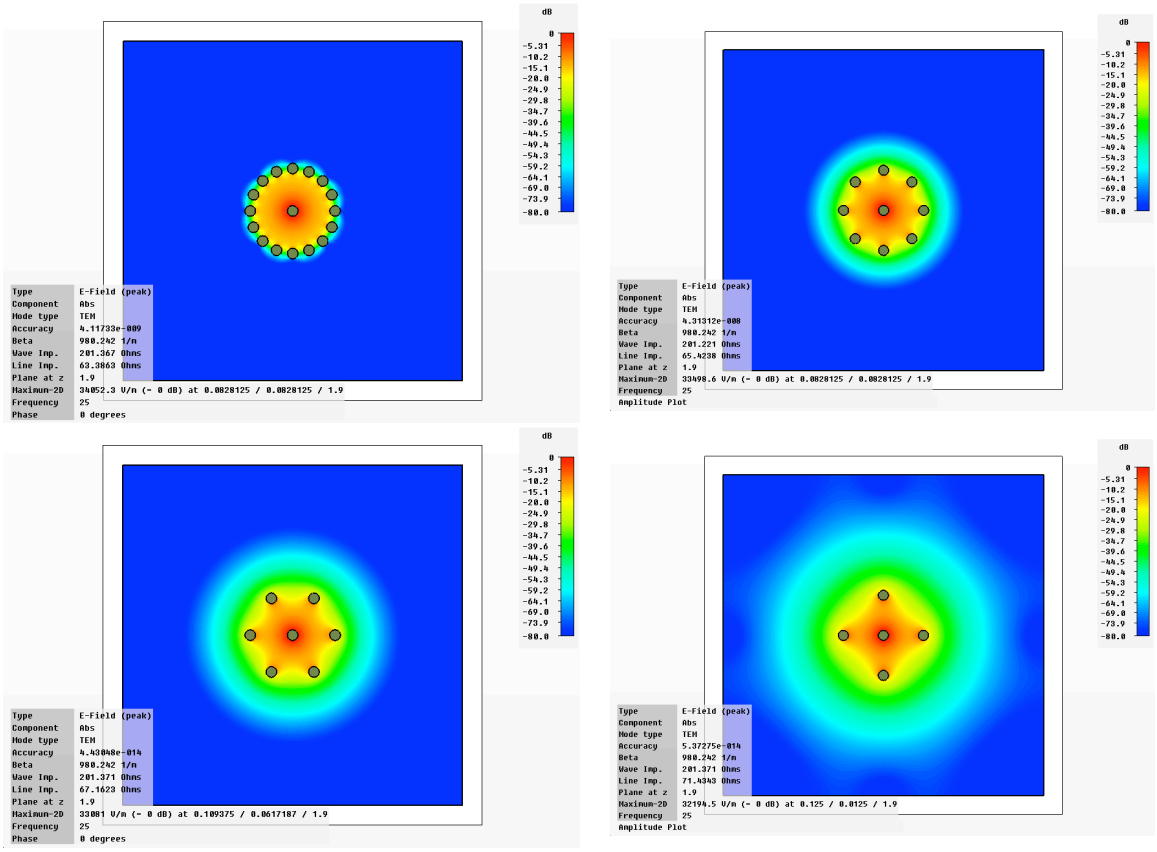

Figure 11 E-field patterns for various ground via configurations at a 1 mm radius. TEM impedance varies from 63.4 to 71.4 ohm. The frequency is 25 GHz.

Figure 12 plots the s-parameters for four ground patterns: four ground vias, six ground vias, eight ground vias (circular), and eight ground vias (square). Cavity resonance modes can be easily observed in the insertion loss plots at 7, 25, 34 and 42 GHz. The insertion loss troughs or "suck outs" correspond to non-localized resonance modes that have been excited by signal energy coupling into the planes. These resonances when viewed as peak E-field distribution of the cavity (Figure 13), show remarkable non-localized energy distribution, which tends to follow a pattern that can be easily seen as a potential to impinge on neighboring signal via arrays.

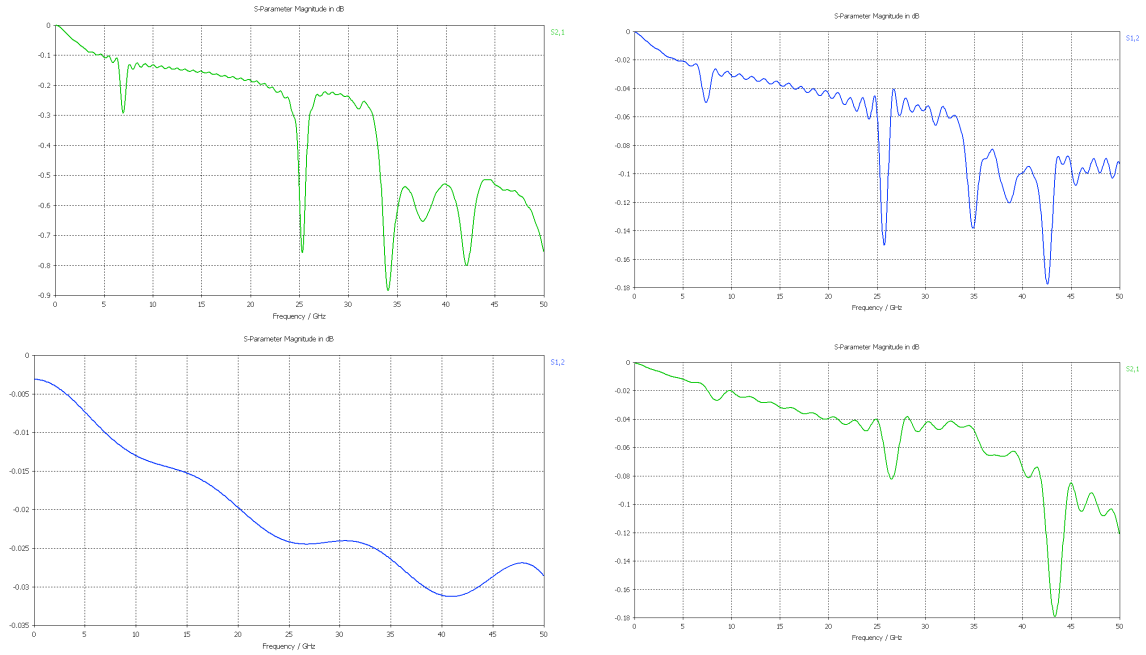

Figure 12 Insertion loss plots show cavity resonance. *Top Left:* 4 ground vias . *Top Right:* 6 ground vias . *Bottom Left:* 8 ground vias. *Bottom Right:* 8 ground vias in square pattern.

In package design, 1.27 mm, 1 mm, and 0.8 mm pitches for pads, balls, and via structures, when coupled with via cavity mode excitation, can create the opportunity for regular array structures, that can not only be excited into resonances, but also can create sympathetic resonances, much like crystal glasses vibrating at exactly the same harmonic frequencies. These sympathetic resonances will "skip" across a package, causing a potential for insertion loss suck outs, and even more dangerous crosstalk peaking, which is not predicted by sectional modeling methods.

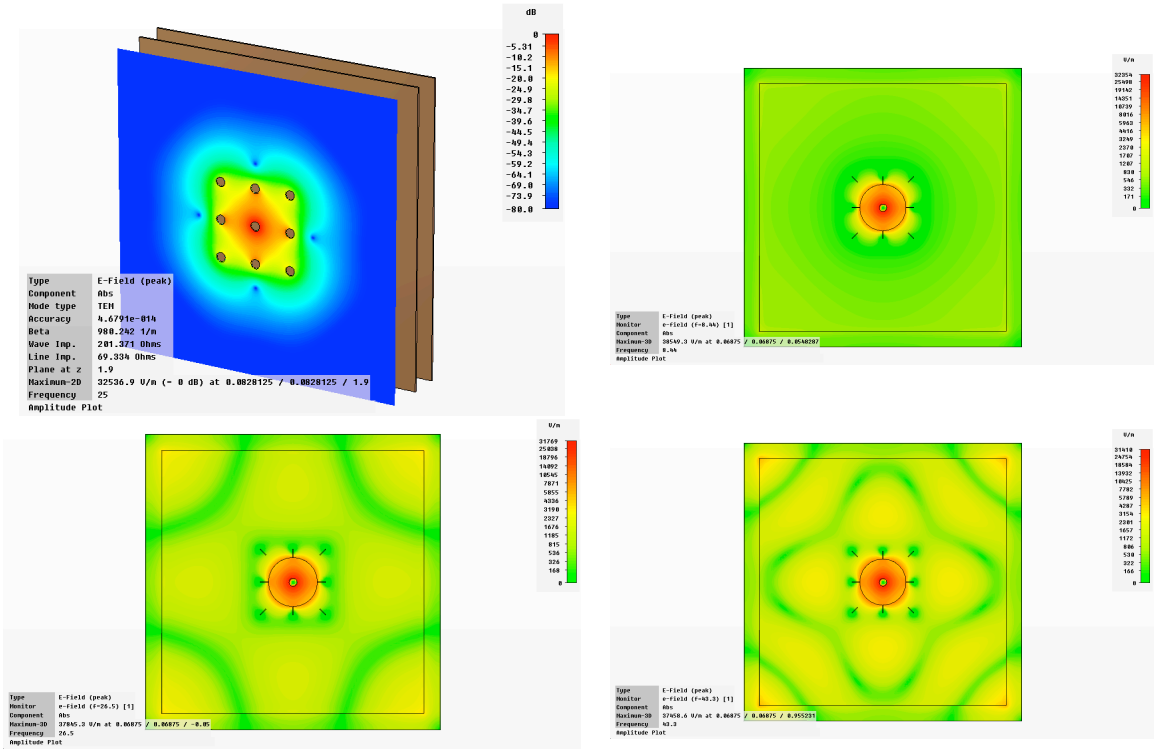

Figure 13 Modal resonance patterns for square pattern of 8 ground vias . *Top Left:* TEM transmission line field . *Top Right:* 8.4 GHz resonance . *Bottom Left:* 26.5 GHz resonance. *Bottom Right:* 43.3 GHz resonance.

4 Simulating Signal-Plane Cavity Interactions

In the following sections we look at different approaches to simulating packages using different field solvers to analyze full packages and truncated packages. We pay particular attention to the impact of boundary conditions.

4.1 Case Study I

A 25 mm x 40 mm package was analyzed to explore the impact of plane cavities on the simulated package s-parameters. The 5-2-5 package has stripline traces routed on two different routing layers above and below the core, referenced to ground. The s-parameters of three differential pairs were extracted using:

1. Ansoft HFSS, truncated model
2. Ansoft SIwave, truncated model
3. Ansoft SIwave, full package model

An open boundary was used in all cases. For Run 1 and Run 2, the package was sliced to include the immediate area surrounding the three differential pairs. The simulation was run only to 15 GHz due to the long solve time of the HFSS model with our available compute resources. The exact same model (including material properties) was used for Run 1 and Run 2. The port implementation differed between Run 1 and Run 2 due to the way the two tools define the ports. Nevertheless, we attempted to make the ports as similar as possible.

Figure 14 shows the single-ended insertion loss for two differential pairs. Immediately, we see the presence of many more resonances in Run 3, which uses the whole package design. In the truncated model we see a smooth and well-behaved insertion and return loss profile that is dictated by the interconnect geometry and losses. Many of the important features shown in Run 3 are missing and furthermore the overall loss is significantly underestimated.

Run 2 shows a resonance at about 12.5 GHz that is most probably a *false* resonance caused by the truncated plane boundary. Just to be clear: unless we purposely adjust the boundary condition to eliminate plane resonances (see Section 4.3) the influence of the plane boundary will be included in the simulation. If the plane boundary is artificial due to a truncated package, for example, any resulting resonances are non-physical – we call these false resonances. If, instead, we simulate the entire package, any plane resonances based on the true package geometry are important to capture and improve our modeling accuracy.

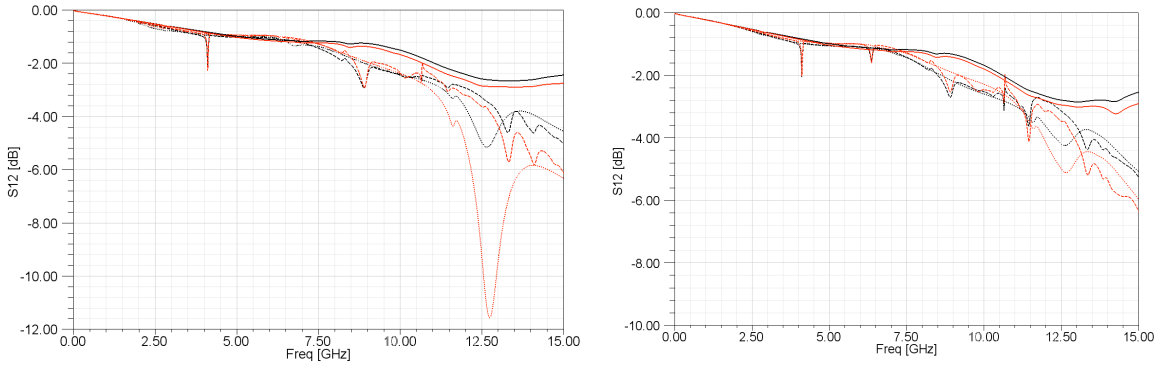

Figure 14 Full package versus truncated package simulation results. Single-ended insertion loss for Rx[0] (*Left*) and Rx[1] (*Right*) simulated using Run 1 (Solid), Run 2 (Dotted) and Run 3 (Dashed).

Cavity resonances can quite often have a significant impact on crosstalk in packages (Figure 15). This is because localized crosstalk to nearest neighbors can often be quite low due to the route separation and ground isolation. This makes crosstalk very sensitive to resonances since very little energy is required to see a big change. As a consequence of cavity resonances, it is not uncommon to see crosstalk peaks associated with these resonances shoot above -20 dB. Moreover, since this crosstalk depends on the cavity resonances, it means this coupling can be non-localized, creating crosstalk between non-

neighboring traces or vias. Notice how Run 1, which neglect cavity resonances, missed the crosstalk peaks entirely and estimates the crosstalk to better than -20 dB.

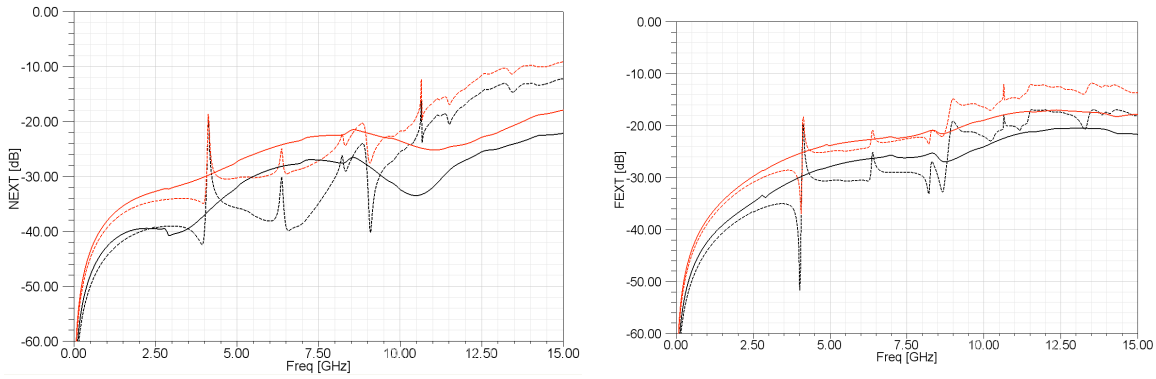

Figure 15 Run 1 versus Run 3 crosstalk simulation results. *Left:* Near-end crosstalk simulated using Run 1 (Solid) and Run 3 (Dashed) for Rx[0]. *Right:* Far-end crosstalk using Run 1 (Solid) and Run 3 (Dashed) for Rx[1].

4.2 Case Study II

A 788 pin flip-chip ball grid array (BGA) was both measured and simulated. The build-up package construction has two routing layers, one above and one below the core. The signals are routed in a stripline configuration referenced to both power and ground.

Single-ended VNA measurements were made using two-sided picoprobes at the bump and balls after a wafer SOLT calibration was made at the probe tips. The ball area was reworked such that a 250 um pitch probe could be utilized at the bump and the ball (see Figure 16 (Left)). The substrate was measured with a Agilent E8363B VNA from 10 MHz to 40 GHz.

The entire package was simulated with Ansoft SIwave. The simulation to measurement correlation is shown in Figure 16 (Top Right). The overall s12 trend is captured nicely including the location of many of the key resonances. Sources of error, which may explain the discrepancies in Figure 16 between measurement and simulation, include material properties, manufacturing differences and tolerances, and the ball rework area (which was not captured in simulation).

Both the simulation and measurement data show a dip at 4 GHz. By running additional simulations and increasing the width of all of the power and ground planes we were able to move the 4 GHz resonance to a lower frequency. Figure 16 (Bottom Left) shows the results of extending the plane width by about 50% (Red). In Figure 16 (Bottom Right) we see that the 4 GHz resonance has moved to a lower frequency (Red). Notice also that some of the resonances in Figure 16 (Bottom Left) remain fixed (e.g. 5.25 GHz and 8 GHz) – many of these resonances are due to discontinuities in the interconnect path.

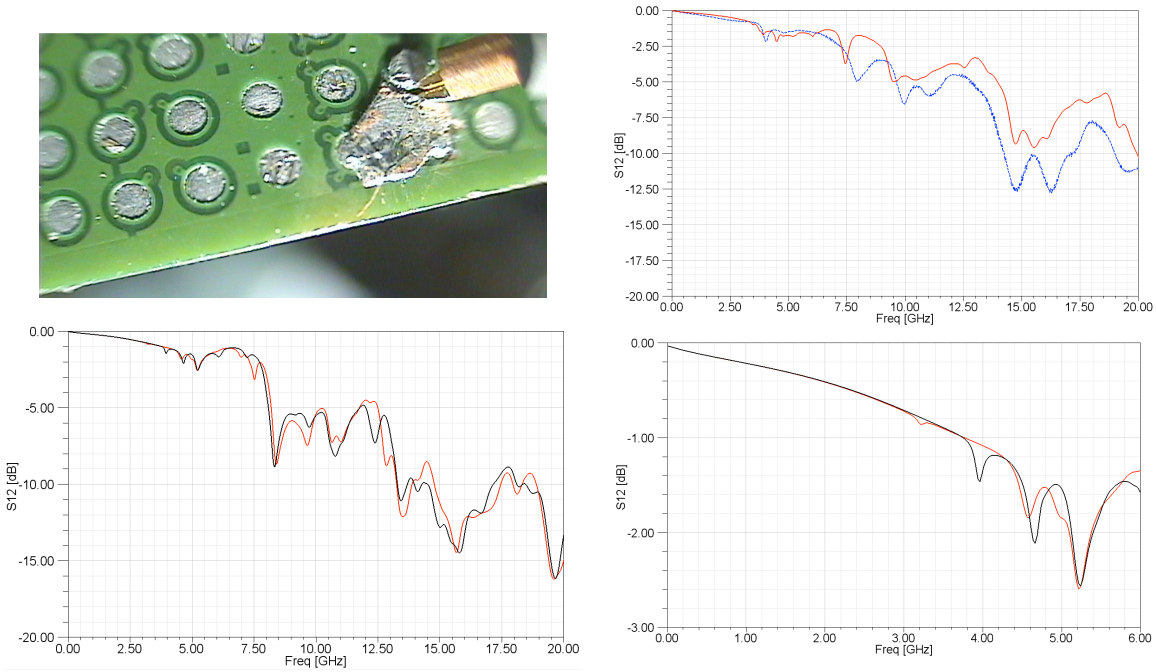

Figure 16 Case Study II results. *Top Left:* Photo of the reworked ball area with the 250 um probe landed. *Top Right:* Insertion loss of the measured (Dashed Blue) and simulated (Solid Red) Trace. *Bottom Left:* Impact of extending all of the planes (Red). *Bottom Right:* Zoom of 4 GHz resonance.

4.3 Impact of Boundary Conditions

It's important to realize that energy injected into a cavity by a via will propagate in all directions and often times, this energy reaches the boundary of the structure. Thus different boundary conditions on electromagnetic simulators will produce very different results.

To illustrate the impact of boundary conditions, a single package trace was simulated using different boundary conditions. Figure 17 shows the rectangular plane structure that was simulated. In a typical package, the plane outlines are much more irregular, dictated by the layout requirements. Here we simplify the problem. Imagine that the longer plane dimension (y-axis) represents the true extents of the plane. Following the procedure outlined in Section 1, a typical package model may be extracted by truncating the longer plane dimension. This case will be explored below.

The package stackup consists of an upper and lower stripline routing layer and a core region separating them vertically. A single signal via and one ground return via provide the vertical connectivity. Modified lumped ports were used on the trace ends [3] instead of waveports because waveports require the radiation boundary to be flush with the port; here we wanted flexibility with offsetting the boundary from the plane edge. A low-loss dielectric (Df=0.01) was used in the core region to allow us to more easily identify the

cavity resonances. Ansoft HFSS was used for the simulations to allow us total flexibility with the boundary conditions.

Different boundary conditions were applied to the mock package structure:

1. x-y-z open boundary
2. x-y-z absorbing boundary
3. x-y open boundary; z absorbing
4. y-z open boundary; x absorbing (on port face)
5. x-z open boundary; y absorbing

An *absorbing boundary* means that an absorbing boundary abuts the plane edge; essentially all fields that arrive at this interface will be absorbed by the boundary condition (i.e. not reflected). An *open boundary* means that the absorbing boundary is pulled back from the plane edge. Fields encountering the plane edge (using the pulled-back absorbing boundary) will be partially reflected and partially transmitted (i.e. radiated into the surrounding medium). In these simulations the boundary condition was not pulled back sufficiently from the structure to avoid all of the fringing fields from being absorbed by the boundary. This was done to improve solve time. The point here is to see the presence of the reflection, not to accurately simulate the reflection.

Figure 17 shows the results for Case 1; we see that the open boundary in all directions allows the plane resonances to be established. The surface plots show the two reflection peaks in the s-parameter data correspond to plane resonances established by the plane boundary.

Figure 18 (Top Left) shows the s-parameter data for the same structure but with the boundary conditions defined by Case 2. Notice that the sharp peaks in the s12 and s11 data are absent as the absorbing boundary does not allow any cavity resonances to be developed. If this type of boundary is applied to a package model, the plane resonances would be missed entirely. Models are commonly simulated using this boundary condition. Note that this boundary condition may be a good choice (in terms of accuracy), as opposed to Case 1, ***if*** the plane has been truncated. Otherwise, artificial open boundaries and plane reflections would be introduced into the problem.

Figure 18 (Top Right) shows the s-parameter data when only the z-axis (vertical) has absorbing boundary conditions. This is another common boundary condition that is used for models; it is assumed that the fields are contained by the outer plane of the stripline and that having the open boundary on the x-y plane, fringing fields and modal resonances would be captured. What we see in the Figure is that Case 3 does modify the cavity resonances although the resonances still appear in the s-parameter data.

The final row in Figure 18 shows the s-parameter data for Case 4 and Case 5. Case 4 is a common boundary condition used in conjunction with wave ports. A requirement of wave ports is that they be flush with the radiation boundary. We see that by doing this we suppress the cavity resonances since the standing waves cannot be established along the

edge that is absorbing. However, notice that there are some differences between Case 4 versus Case 5: Case 5 shows some broader resonances in the response. This is because as the plane wave propagates radially out from the via, it encounters *less* absorption in Case 5 as compared to Case 4.

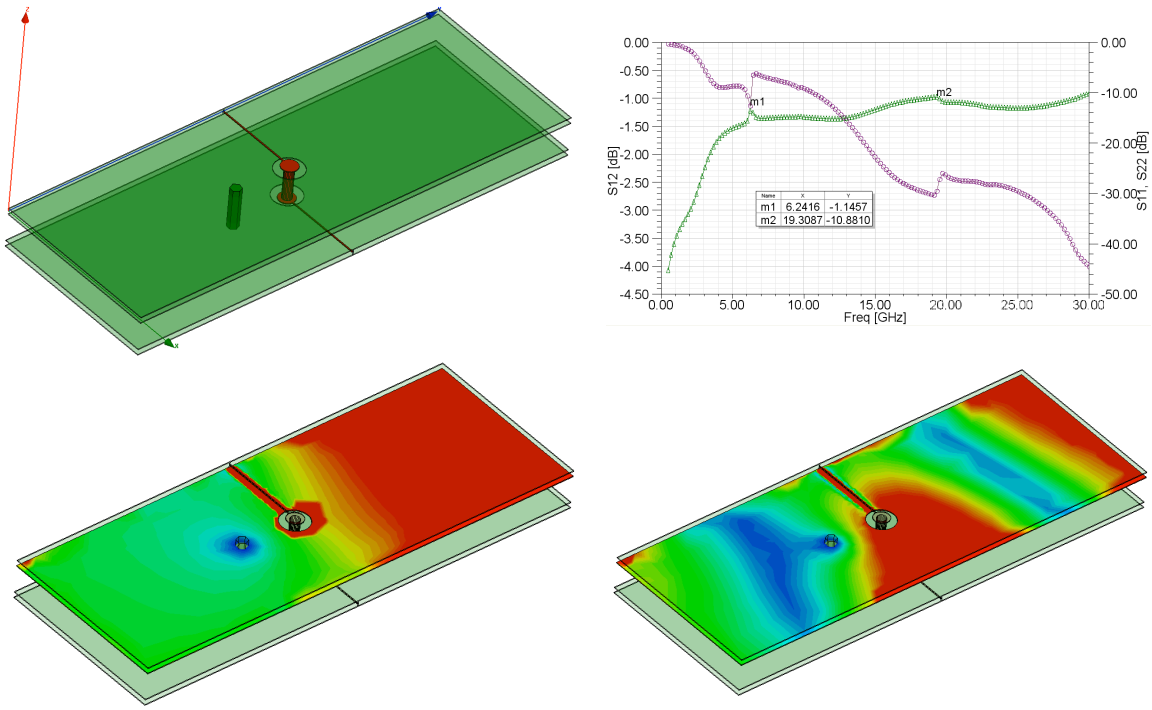

Figure 17 Single package trace simulation. *Top Left:* Problem geometry. *Top Right:* Simulated s-parameters for Case 1. *Bottom Left:* Voltage surface plot at 6.2 GHz. *Bottom Right:* Voltage surface plot at 19 GHz.

In a typical package model extraction, the long dimension of the plane (y-axis) in Figure 17 would be truncated, creating a narrow strip around the package trace. To illustrate the impact of this, Figure 19 (Left) shows the simulation results for Case 1 with a 3 mm and 8 mm plane width (8 mm is pictured in Figure 17). We see that the modal resonances have shifted to a higher frequency when the plane is truncated. If this was a real package design, non-physical resonances would be introduced by truncating the plane. On the right of Figure 19 we simulate both plane widths but for Case 2. Although there are some differences, we see that this boundary condition makes these two cases look very similar.

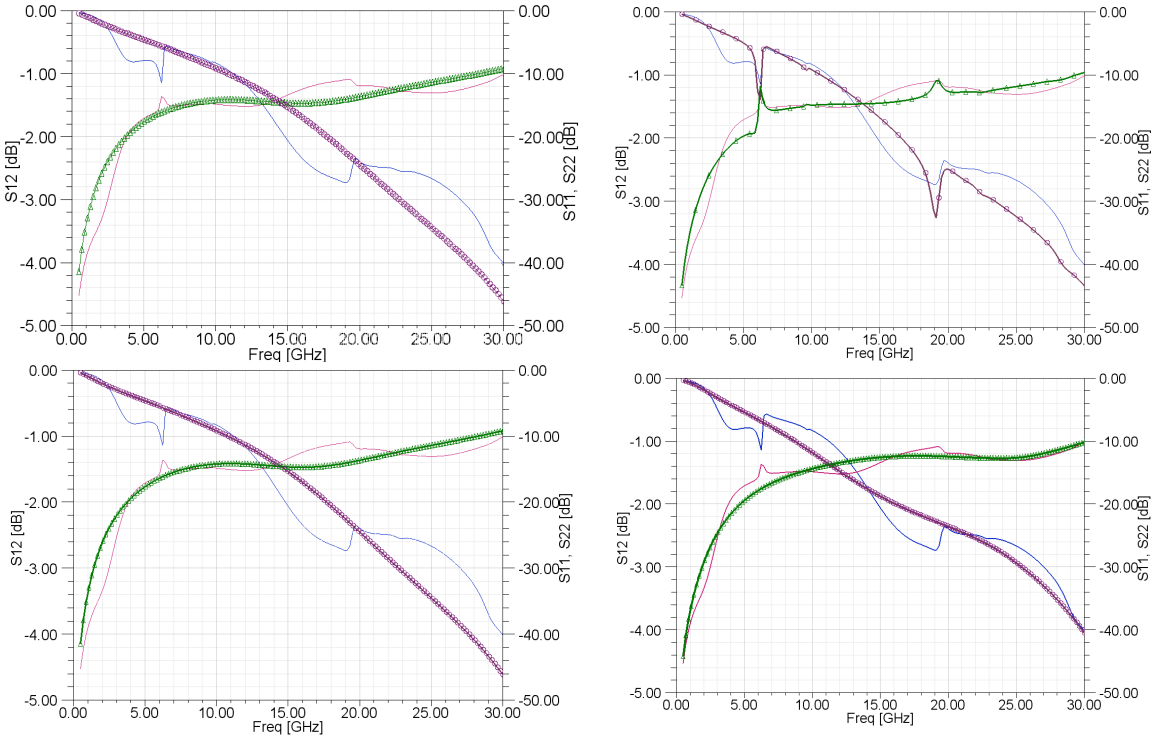

Figure 18 S-parameter plots of the single package trace using different boundary conditions. *Top Left:* Case 2 (Symbols) versus Case 1 (No Symbols). *Top Right:* Case 3 (Symbols) versus Case 1 (No Symbols). *Bottom Left:* Case 4 (Symbols) versus Case 1 (No Symbols). *Bottom Right:* Case 5 (Symbols) versus Case 1 (No Symbols).

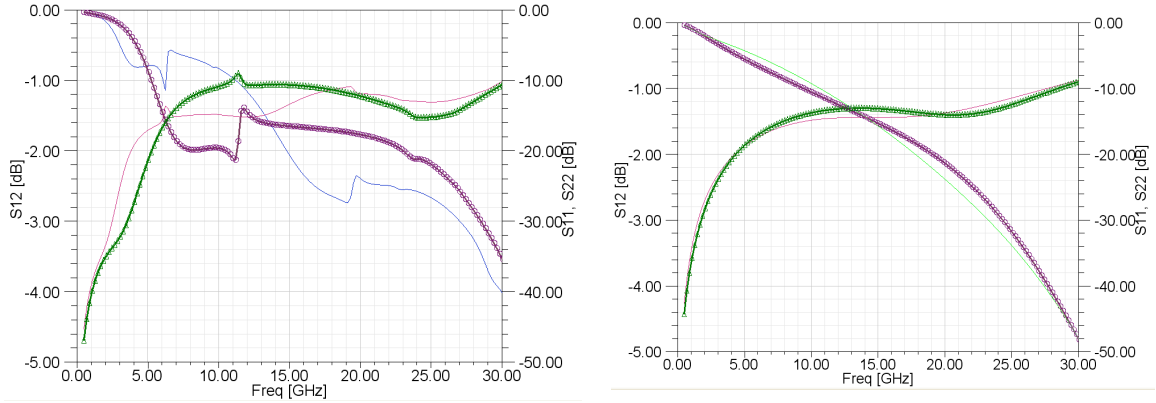

Figure 19 S-parameter plots of the single package trace using different plane widths. *Left:* Case 1, 3 mm wide (Symbols) versus Case 1, 8 mm wide (No Symbols). *Right:* Case 2, 3 mm wide (Symbols) versus Case 2, 8 mm wide (No Symbols).

5 Coupled Differential Via Correlation

This paper heavily relied on Ansoft SIwave for many of the simulations. As such it is important to correlate the simulator to measurements.

A suite of structures were designed by Teraspeed Consulting for the identification of material parameters of package dielectrics and for benchmarking various electromagnetic and signal integrity simulators using advanced VNA measurement techniques. There are 19 test structures on the board, comprising calibration structures, transmission line segments, and resonant structures, in addition to typical elements of single-ended and differential multi-gigabit package data channels. All test structures are equipped with optimized transitions from 2.92 mm edge-launch connectors to microstrip and stripline lines that minimize measurement impedance discontinuities and extend the effective measurement bandwidth to 40 GHz. These transitions were designed to have a modal cutoff frequency of 55 GHz, well beyond the measurement bandwidth of the VNA.

For the purposes of correlating Ansoft SIwave and for this study, one of the test structures was simulated and measured. This structure consists of coupled differential vias. There are eight 2.92 mm edge-launch connectors on the board, one for each port of the two, coupled differential vias. The top view of the structure is shown in Figure 20 (Top Left) and a zoom of the via region on the Top Right.

An Agilent E8363B 40 GHz 4-port network analyzer was used to measure S-parameters of the on board TRL calibration kits, and for subsequent measurements of all test structures. The impact of measurement cables, SMA connectors, connector-to-trace transitions, and lead-in traces are de-embedded from the measurements using TRL calibration techniques, yielding accurate measurements of the structures under test.
To facilitate numerical modeling and simulation of the test structures, per-unit-length insertion loss and phase curves were calculated using the method of generalized modal S-parameters [6]. Dielectric and conductor material models used in the solvers were then fit to the Djordjevic-Sarkar [7] dielectric loss model, and to the Hammerstad-Jensen copper surface roughness model [8], using a heuristic approach with each target solver. All subsequent numerical modeling, simulations and correlations to measurement were performed with these heuristically extracted values as a starting point.

The correlation is shown in Figure 20 for the insertion (Bottom Left) and return loss (Bottom Right). We see good correlation between the measured and simulated data: the slope of insertion loss is captured along with the null locations and peaks in the return loss profile. With this correlation established, the structure served as the basis for many of the simulations in this paper, with some slight modifications. Specifically, the simulations used to generate Figure 2 through Figure 8 were performed using modified versions of the structure shown in Figure 20. The solvers settings were also maintained after the correlation was established. This methodology improved our confidence with the simulation runs.

Finally notice that there are no identifiable plane resonances observed in Figure 20 despite the fact that the plane is large and the core is not heavily stitched with ground vias. This is because of the large losses in the trace. Referencing Eq. (2), the dissipative losses reduce the amount of radiative losses.

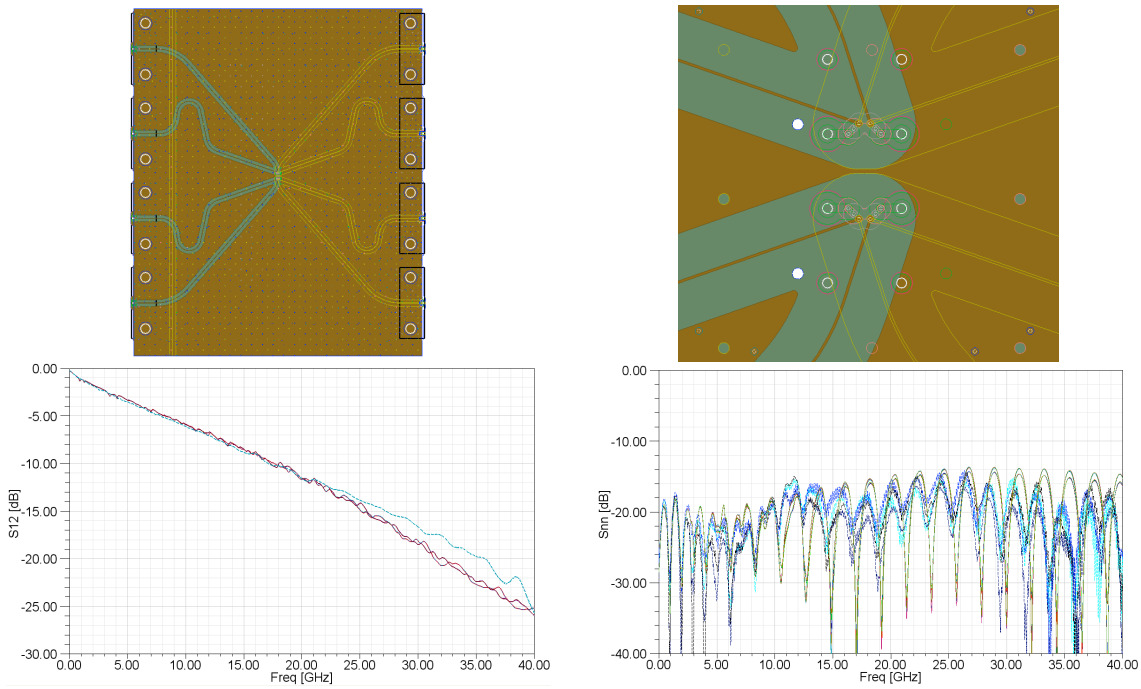

Figure 20 Coupled differential via correlation. *Top Left:* Full imported test board. *Top Right:* Zoom of via region. *Bottom Left:* Insertion loss (Dashed Blue is measured). *Bottom Right:* Return loss (Dashed Blue traces are measured).

6 Conclusions

In this paper we have shown how vertical transitions can excite cavities and that the resulting cavity resonances have a significant impact on the signal loss, crosstalk and return loss. Moreover, we have shown that depending on how the model was created and the boundary conditions used, these resonances may or may not be captured.

One solution to this problem is to carefully manage the return path of the vertical transition such that very little energy is introduced into the cavity. This not only prevents the excitation of cavity resonances but it also limits the computational volume since the region outside of the return path would be isolated. We showed the limitations of this approach and showed how these current containment methods may introduce new resonances.

We showed that if the vertical transition is not carefully managed, it may be necessary to analyze not only the signal path but the entire power ground network, including cavities. We found that hybrid solvers can be a good choice in analyzing this type of problem. In

general, hybrid solvers attack the problem by dividing the problem into different geometry types (i.e. traces and metal shapes) and decomposing the problem into two fundamental modes: the parallel plate node and the transmission line mode. Approaching the problem this way has a significant advantage compared to meshing the entire volume, which requires many mesh cells. Furthermore, because the ratio of the largest mesh cells to the smallest is quite large, an adaptive meshing algorithm is needed to not overload compute resources.

If the modeler must rely on a full-wave solver and, consequently, the plane is truncated to reduce solve time, we showed that it is highly advisable to use absorbing boundaries abutting the plane to avoid false resonances created by the new plane boundaries.

References

1. Jason R. Miller, Gustavo Blando, K. Barry A. Williams, Istvan Novak, "Impact of PCB Laminate Parameters on Suppressing Modal Resonances," Proceedings of DesignCon 2008, Santa Clara CA.
2. Istvan Novak, Jason Miller "Frequency Domain Characterization of Power Distribution Networks," Artech House, 2007.
3. Jason R. Miller, Gustavo J. Blando, Roger Dame, K. Barry A. Williams, Istvan Novak, "Examining the Impact of Split Planes on Signal and Power Integrity," Proceedings of DesignCon 2009, Santa Clara, CA.
4. Gustavo Blando, Jason R. Miller, Douglas Winterberg, Istvan Novak, "Crosstalk in Via Pin-Fields, Including the Impact of Power Distribution Structures," Proceedings of DesignCon 2009, Santa Clara, CA.
5. Istvan Novak, Jason R. Miller, Eric Blomberg, "Simulating Complex Power-Ground Plane Shapes with Variable-Size Cell SPICE Grids," Proceedings of EPEP 2002.
6. Y. Shlepnev, A. Neves, T. Dagostino, S McMorrow, "Practical identification of dispersive dielectric models with generalized modal S-parameters for analysis of interconnects in 6-100 Gb/s applications", Proceedings of DesignCon 2010.
7. Djordjevic, R.M. Biljic, V.D. Likar-Smiljanic, T.K.Sarkar, "Wideband frequency domain characterization of FR-4 and time-domain causality", IEEE Trans. on EMC, vol. 43, N4, 2001, p. 662-667.
8. E. Hammerstad and O. Jensen, "Accurate models for microstrip computer aided design," in IEEE MTT-S Int. Microwave Symp. Dig., Washington, DC, 1980, pp. 407–409.
9. A. E. Engin, K. Bharath, K. Srinivasan, and M. Swaminathan, "Modeling of Multilayered Packages and Boards using Modal Decomposition and Finite Difference Methods," *Proc*. 2006 *IEEE Symposium on Electromagn. Compat.*, vol. 3, pp. 646–650, August 2006